Computational Biology and Chemistry

Incremental Learning for Leukemia Classification Based On Hybrid Deep Learning Using Blood Smear Image

--Manuscript Draft--

Manuscript Number:	CBAC-D-24-00655
Article Type:	Research Paper
Keywords:	Tangent Sand Cat Swarm Optimization; Tangent Search Algorithm; Sand Cat Swarm Optimization; Long Short Term Memory; LeNet
Abstract:	Leukemia is the most common form of blood cancer that caused because of abnormal production of immature malignant cells from the bone marrow. Leukemia is a life-threatening disease that resists the ability of infections by affecting the immunity system of human body and can lead to death, if not treated promptly. Thus, immediate treatments are necessary to detect leukemia at initial stage to control the abnormal cell growth. Leukemia detection from microscopic images of blood smear of malignant leukemia cell is a time-consuming and tedious task. Thus, a Tangent Sand Cat Swarm Optimization-Long Short Term Memory-LeNet (TSCO-L-LeNet) with incremental learning is designed for precise classification of leukemia. Here, the adaptive median filter is used to pre-process the input image and the pre-processed image is segmented using Scribble2label. Later, the augmentation of segmented image is performed and various feature extractors are utilized for the extraction of features from the augmented image. Finally, the L-LeNet with incremental learning is executed for leukemia classification from the extracted features, where TSCO approach is used to train the weights of L-LeNet. The experimental results show that TSCO-L-LeNet achieved maximum performance with 92.65% accuracy, 91.47% True Negative Rate (TNR), and 92.22% True Positive Rate (TPR).

Incremental Learning for Leukemia Classification Based On Hybrid Deep Learning Using Blood Smear Image

[1]Smritilekha Das, and [2*]Padmanaban K

[1]Assistant Professor

Computer Science and Engineering

Koneru Lakshmaiah Education Foundation, Vaddeswaram, AP, India.

[2*]Associate Professor

Computer Science and Engineering

Koneru Lakshmaiah Education Foundation, Vaddeswaram, AP, India.

[2*]padmanabank910@gmail.com

Abstract

Leukemia is the most common form of blood cancer that caused because of abnormal production of immature malignant cells from the bone marrow. Leukemia is a life-threatening disease that resists the ability of infections by affecting the immunity system of human body and can lead to death, if not treated promptly. Thus, immediate treatments are necessary to detect leukemia at initial stage to control the abnormal cell growth. Leukemia detection from microscopic images of blood smear of malignant leukemia cell is a time-consuming and tedious task. Thus, a Tangent Sand Cat Swarm Optimization-Long Short Term Memory-LeNet (TSCO-L-LeNet) with incremental learning is designed for precise classification of leukemia. Here, the adaptive median filter is used to pre-process the input image and the pre-processed image is segmented using Scribble2label. Later, the augmentation of segmented image is performed and various feature extractors are utilized for the extraction of features from the augmented image. Finally, the L-LeNet with incremental learning is executed for

leukemia classification from the extracted features, where TSCO approach is used to train the weights of L-LeNet. The experimental results show that TSCO-L-LeNet achieved maximum performance with 92.65% accuracy, 91.47% True Negative Rate (TNR), and 92.22% True Positive Rate (TPR).

Keywords: Tangent Sand Cat Swarm Optimization; Tangent Search Algorithm; Sand Cat Swarm Optimization; Long Short Term Memory; LeNet

1. Introduction

Cancer is considered the mostdeadly disease and has created various impacts on people worldwide [3]. In 2018, it was reported that the second-largest cause of death worldwide is cancer, where about 18.1 million new cancer cases and 9.6 million people die due to cancer globally [7]. Themost dangerous type of cancer as compared to all types of cancer disease is blood cancer. Leukemia disease is caused due to White Blood Cells (WBC), which is one among blood constituents that comprises about one percent of total blood volume. The platelets and Red Blood Cells (RBCs) are the other blood constituents. The immunity of the human body is mainly based on the count of WBC, which helps to fight against infectious and harmful diseases. The bone marrow of the human body is affected by leukemia that destroys the immunity of the human body [3]. The Greek word “leukos” indicates “white” and “aim” represents “blood” is the entomology of leukemia [5]. Leukemia is generated from bone marrow and distributesan excess amount of leucocytes in blood uncontrollably [6]. The large number of immature leukocytes leads to the generation of leukemia [3]. Generally, leukemia generates in the form of WBC but in certain cases, it also originates in other types of blood cells. Leukemia is mainly classified based on its chronic (slower-growing) or acute (fast-growing) characteristics [2].

Generally, chronic leukemia is the slow growth of the disease and the rapidgrowth of the disease is termed as acute leukemia. Chronic leukemia shows more severe symptoms as compared with the symptoms of acute leukemia [3]. Acute leukemia is also classified into different types, namely Acute Lymphoblastic Leukemia (ALL) and Acute Myeloid Leukemia (AML). The ALL is a form of blood cancer that affects the lymphocytes of cells to create lymphoblasts, which also leads the patient to death by degrading the immune system of the human body. ALL creates a high risk of survival among children below five years and adults more than 50 years old [8]. ALL begins from bone marrow which is responsible for the origination of new blood cells. The leukemia cells quickly invade human blood most often through which it also spreads to other parts of the human body including the testicles, central nervous system, spleen, liver, and lymph nodes [2]. The survival rate of patients suffering from ALL is about 3 months, if necessary treatments are not provided to patients on time [3]. Based on the statistical reports collected about ALL, about 5690 new ALL cases were determined only in the United States in 2021 out of which about 1550 people including adults and youngsters are anticipated to die. ALL is completely curable when diagnosis is provided to affected patients at early stages [4].

The symptoms of leukemia are more similar to the symptoms of other diseases, such as bone pain, weakness, fever, joint pain, and anemia [4]. Thus, accurate therapy and treatment play a vital role in saving the life of a patient [3]. In recent years, ALL diagnoses required a well-experienced pathologist to perform microscopic analysis on blood smears by taking a biopsy of bone marrow [6]. The blood samples are collected by spreading and staining the blood as a thin layer in a microscope slide forming a blood film, which is also termed a blood smear [1]. However, the manual detection of leukemia suffers from different issues, like the complex nature of blood cells, weak edges, blur, and noise, and is also highly reliant on human interpretation [3]. The commonly utilized approach to screen patients with ALL

initially is visual analysis of microscopy images, but it is a very time-consuming and subjective task [5]. At present, computer vision and image processing-based approaches are utilized to eliminate the errors caused due to human factors [4]. The advancements of deep learning techniques helps to accurately detect leukemia disease and allow doctors to properly diagnose the disease based on its conditions. The common procedure followed during the classification of leukemia involves image pre-processing, feature extraction, selection, as well as classification [3]. Several algorithms and approaches are adopted for medical image analysis which also performs both classification as well as feature extraction tasks to yield best performance [8].

This paper presents a deep learning model TSCO-L-LeNet with incremental learning for accurate leukemia classification from blood smear images. Initially, the pre-processing of input blood smear image is executed by using adaptive median filter. Afterward, the Scribble2label is used for the segmentation of pre-processed images. Later, the augmentation of the segmented blood smear image is executedby utilizing different augmentation process, like flipping, rotation, scaling, and color augmentation. Then, various feature extractors are utilized for the extraction of features from the augmented blood smear image. Finally, the classification of leukemia is carried out based on the extracted features using the L-LeNet model, here the TSCO algorithmic technique is used to effectively tune the weights of L-LeNet. Moreover, incremental learning is performed on the classified leukemia output for incremental learning and the weights are bounded using holoentropy.

The major contribution of the research is,

- ***DesignedTSCO-L-LeNet for Leukemia classification****:* The TSCO-L-LeNet model is designed with incremental learning for earlydetection ofleukemia from blood smear images. Here, L-LeNet is designed by incorporatingLeNet and Long Short-Term Memory (LSTM) models. The optimal weights of L-LeNet are effectively fine-tuned

using the TSCO algorithmic approach, where TSCO is introduced by integrating Tangent Search Algorithm (TSO) and Sand Cat Swarm Optimization (SCSO).

The article is organized as, the analysis of traditional literature utilized for leukemia classification is portrayed in section 2 and the TSCO-L-LeNet approach and incremental learning designed for leukemia classification are elucidated in section 3. In addition, in section 4, the outcome of the investigation and discussions that are followed is demonstrated and section 5 enumerates the conclusion of the manuscript.

2. Motivation

In certain cases, the leukemia may cause death if accurate treatments are not provided early. In general, various numbers of invasive disease analysis techniques are employed for early diagnosis of leukemia disease. However, these techniques are tedious, error-prone, and burdensome during the classification of leukemia. Thus, it encourages to introduce a novel deep learning model for the early classification of leukemia from blood smear images.

2.1. Literature Review

Al-Qudah, R. and Suen, C.Y., [1] developed enhanced incremental training for the classification of WBC and platelet subtypes as well as morphological abnormalities. In this model, the confusable classes were handled effectively and the classes were classified into morphological abnormalities as well as subtypes from the synthetic blood smear database. It classified both the normal and huge platelets as one class and also reduced the misclassification rate of the model, but the model was not suitable for the large-scale non-medical and medical database. Ramaneswaran, S., *et al.* [2] designed Inception v3 XGBoost for accurate classification of ALL from images of WBC. Here, the Inception v3 XGBoost was employed as the classification head, and was used to extract image features. This

approach was highly reliable in detecting ALL cells, but it failed to learn spurious features that caused data leakage problems. Sulaiman, A., *et al.* [3] introduced the ResNet Random Support Vector Machine (ResRandSVM) approach for the classification of ALL from blood smear images. This approach utilized feature selection techniques using feature encoding networks for the extraction of deep features from the blood smear images. The generalization capability of the technique was improved during image classification by capitalizing the strength of each component. However, this model failed to increase accuracy by integrating machine learning and deep learning algorithms. Zakir Ullah, M., *et al.* [4] established the Efficient Channel Attention-Visual Geometry Group (ECA-VGG16) for the classification of ALL by extracting high-quality image features from the database. This approach increased the balancing among the classes thus effectively overcoming overfitting issues, but it was not successful for multi-class classification of similar diseases from different databases.

Rodrigues, L.F., *et al.* [5] designed a Genetic Algorithm (GA) for the classification of ALL from microscopy images. It effectively improved the detection rate between healthy and immature lymphocytes. This technique utilized less computational resources while classifying leukemia, but the model required more computational time to perform optimization task. Saeed, U., *et al.*[6] developed a CNN-based deep learning model for the detection of ALL. Here, the images from the actual database were generated by utilizing different data augmentation approaches. It effectively handled overfitting issues that occurred during the testing and training process during ALL classifications. However, it failed to increase the performance by utilizing Generative Adversarial Network (GAN) and was not successful for multi-classification of images using pre-trained models. Baig, R., *et al.* [7] introduceda CNN model for the detection of ALL, AML, and Multiple Myeloma (MM) from the blood smear images. It obtained dense features by removing non-essential blood supplies and also, performed segregation for the categorization of classes into malignant and non-

malignant. The execution time of the whole system was minimized during classifying the input images. However, the technique was not successful for leukemia classification using real-time databases. Das, P.K. and Meher, S., [8] established a CNN model for ALL detection by effectively analyzing the medical images. In this approach, high precise results are obtained by employing residual transfer learning networks. This approach effectively avoided problems that occurred due to vanishing gradients during the detection and classification of ALL. However, the model delivered poor performance while using splitted database for classification.

2.2. Challenges

The limitations addressed by prevailing schemes utilized for leukemia classification are enumerated as follows,

- The enhanced incremental training model used in [1] effectively handled the visual resemblance during the classification of platelets. However, it was not successful in analyzing blood smear images in real-time applications and the model required extra efforts to correct the results with high priority.
- The Inception v3 XGBoost approach used in [2] recorded less computational time for the classification of leukemia, but it failed to pay attention to the regions surrounded by cells as well as redundant parts of the cell image for leukemia classification.
- The ResR and SVM technique used in [3] significantly captured more complex patterns and enabled highly effective discrimination among various classes. However, the model was computationally expensive in classification for large databases with more features.

- The ECA-VGG16 model employed in [4] converged quickly while categorizing healthy and ALL cell images, but it failed to reduce the total false positive rate to increase the performance of the model.
- The traditional classification techniques provided cost-effective, safe, and faster solutions while classifying ALL. However, the approaches required human experts for analyzing huge databases that consists hundreds and thousands of medical blood smear images. It also faced difficulties to automatically classify leukemia disease by determining the morphological similarity among blast immature leukemic and normal cells.

3. Designed TSCO-L-LeNet with incremental learning for classification of Leukemia from blood smear image

In this research, TSCO-L-LeNet is introduced and incremental learning is performed for classification of leukemia using blood smear image. Initially, the input blood smear image is from the database and is pre-processed using an Adaptive median filter [9]. Then, the cell segmentation is performed by using Scribble2label [10] and the image augmentation is performed in the segmented image by flipping, scaling rotation, and color augmentation [21]. After image augmentation, the feature extraction is performed for the extraction of statistical features such as mean, median, standard deviation, variance, skewness, kurtosis, CNN features [24], GreyLevel Co-occurrence Matrix (GLCM) features [11]: Contrast, correlation, energy, homogeneity, and entropy, Complete Local Binary Pattern (CLBP) [12], Pyramid Histogram of Oriented Gradients (PHOG) [13], Local Vector Pattern (LVP) [14] and Local Gabor XOR Patterns(LGXP) [15].Later, the L-LeNet is employed for the classification of Leukemia, where the designed L-LeNet is the integration of LeNet [16] and LSTM [17]. The optimal weights of L-LeNet are fine-tuned using TSCO. The algorithmic approaches, TSA

[18] and SCSO [19] are incorporated to obtain the TSCO model. Similarly, the incremental image at a time 't' and '$t+1$' is performed to the leukemia classifier for incremental learning. From this, at the time 't' the error produced in the leukemia classifier is an error (e^t) and for incremental image, at the time '$t+1$' the error produced is e^{t+1}. Later, the errors are compared and if the error e^{t+1} is greater than (e^t) then the weights are bounded by using holoentropy. Figure 1 elucidates the schematic view of TSCO-L-LeNet with incremental learning for leukemia classification using blood smear image.

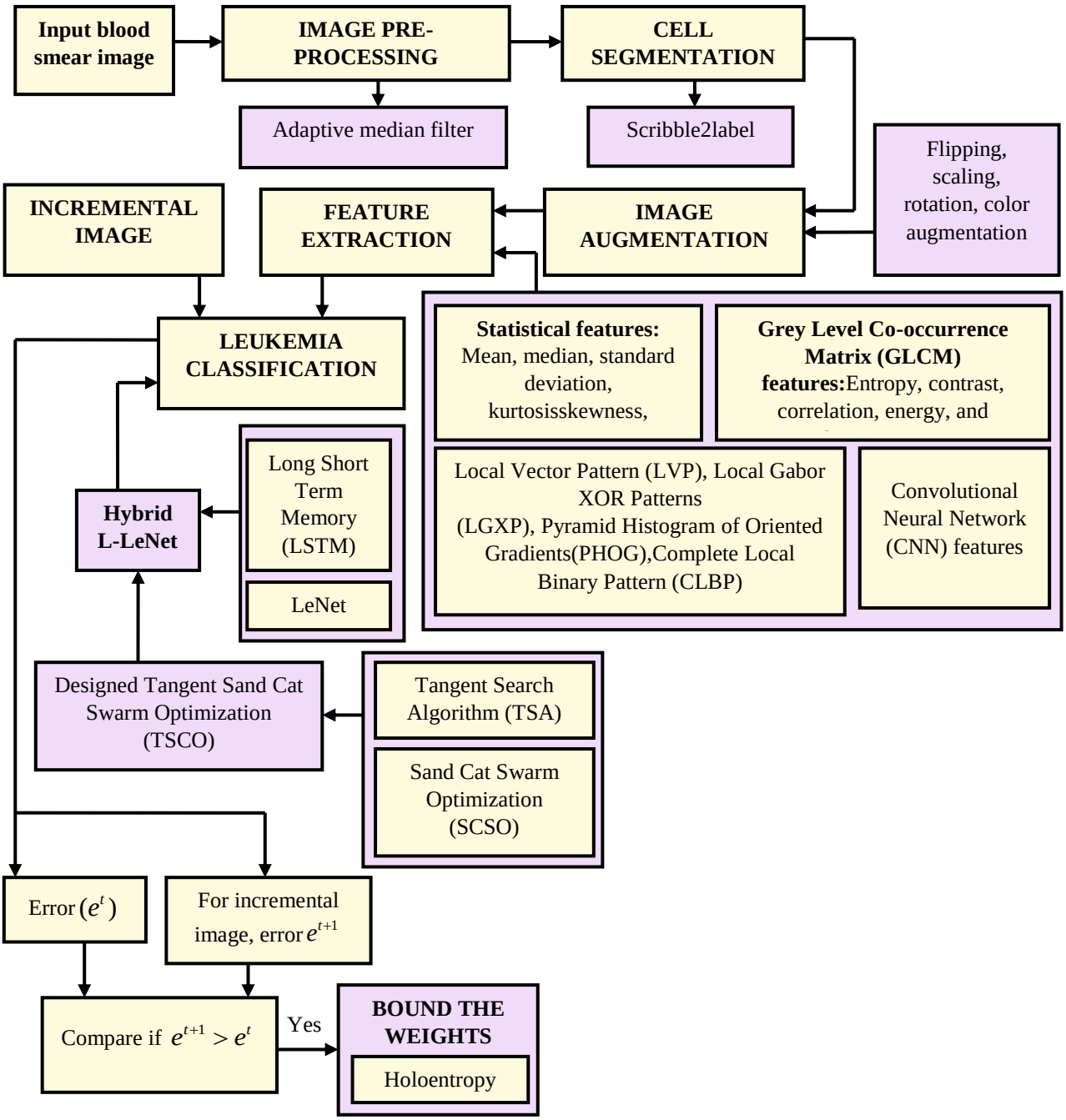

Figure 1. Schematic view of TSCO-L-LeNet with incremental learning for the classification of leukemia using blood smear image

1) Acquisition of image

Initially, from the Blood Cells Cancer (ALL) database, the input blood smear image is taken for classification of leukemia, which is designated as,

$$W = [W_1, W_2, W_3, ..., W_E, ..., W_R] \quad (1)$$

where, W represents the Blood Cells Cancer (ALL) dataset taken for leukemia classification, W_E indicates the E^{th} blood smear image considered for leukemia classification, and R signifies total number ofblood smear imagespresentedin the Blood Cells Cancer (ALL) dataset.

2) Image pre-processing

The blood smear image W_E taken for the leukemia classification is pre-processed initially for the elimination of naturally presented noises. Here, the pre-processing of the blood smear image is performed using an adaptive median filter [9]. Generally, adaptive median filters are more sophisticated as compared with classical median filtering approaches. It helps to reduce distortions, smooth other noises, and remove impulse noises from the blood smear image. It effectively identifies the image pixels that are affected by impulse noise via spatial processing. It compares each pixel to its neighbor to determine the noise presented in the image pixel. The deviated pixel that is not identical to majority of neighbours is determined as noise. Thus, during pre-processing of input blood smear image W_E, the resultant pre-processed output T_P is obtained and is sent to the cell segmentation phase.

3) Cell segmentation

In general, segmentation is performed to extract Region of Interest (ROI) from the imagefor quantitative analysis. Accurate cell segmentation is necessary during leukemia classification

for the detection of the shape and nature of immature or blast cells. The pre-processed image T_P is fed into Scribble2label [10] for cell segmentation, where the pre-processed blood smear image T_P and scribbles α provided by the user are the input sources used for cell segmentation in Scribble2label. It is used to effectively generate training labels under less computational time by reducing manual efforts.The input scribbles are taken as labelled pixels and the other pixels are considered as unlabeled pixels. A standard cross-entropy loss is generally allowed to labeled pixels and during training, the predictions of exponential moving average are used to create reliable labels automatically for unlabeled pixels. The Scribble2label is trained under two distinct stages, such as initialization and learning of self-generated labels. In the first stage, the scribbled pixel loss is used to train the model. Then, both unscribbled and scribbled losses are performed to refine the prediction more iteratively, once the model is trained during initialization.

For input training data, a user-drawn scribbles set is taken, which effectively trains the model in the first few iterations and creates average predictions. The user-drawn scribbles arethe subset of corresponding mask annotation, and cross entropy loss is utilized by the model to eliminate the unscribbled pixels, which is expressed by,

$$\beta_{SP}(T_P,\alpha) = -\frac{1}{|\Omega_\alpha|}\sum_{a=\Omega_\alpha}\left[\alpha_a \log\left(f(T_P;\theta_b)\right) + (1-\alpha_a)\log\left(1-f(T_P;\theta_b)\right)\right] \tag{2}$$

where, T_P indicates pre-processed blood smear image, the scribble annotation is indicated as α, the scribbled pixel set is denoted as Ω_α, θ_b denotes network parameter, and the prediction of the model at b^{th} iteration is symbolized as $f(T_P;\theta_b)$. The initialization is continuously performed till achieving the warm-up epoch P_i. In addition, the prediction's exponential moving average is estimated periodically duringthe training process. Once the best model is determined, the predictions cannot be ensembled in the scribble supervised setting due to non availability of fully annotated labels. The computational cost is reduced

and a valuable ensemble is achieved by the model by averaging the predictions at every ensemble interval. Thus, the final cell segmentation output T_S is obtained during the segmentation using Scribble2label.

4) Image augmentation

The final cell segmentation output T_S is allowed for image augmentation to effectively overcome overfitting issues and to randomly transfer image samples to improve diversity. The various image augmentation process, such as color augmentation, rotation, scaling, and flipping are applied in cell segmentation output T_S . The augmentation process performed by the method is briefly illustrated as follows,

-Flipping: The flipping [21]is used to reflect the segmented image T_S around both horizontal and vertical axis or horizontal or vertical axis. It helps to improve the total number of images available without using any artificial applications and A_F signifies the resultant flipped augmented image.

-Scaling: It is the method used to magnify the segmented images T_S , which is used to scale the image to its actual size and also helps to cut the image from the initial x and y location to another x and y location [21]. The resultant scaled augmented image A_S is obtained while scaling the segmented image T_S .

-Rotation: It is a traditional geometric image augmentation technique [21] and is applied in an additive way to the segmented image T_S . The segmented image T_S is rotated near the axis along left and right direction between1 and 359 degree angles and the final rotation augmented output A_R is obtained

-Colour augmentation: During color augmentation [22], the images are split into blue, green, and red bands to change the color of the segmented image T_S . The green, green, and

red bands are utilized after reassembling the image. Thus, various colors are obtained, and the resultant color augmentation image is specified as A_C.

Therefore, the results obtained during the augmentation of the segmented image T_S are finally expressed as,

$$A_{AU} = [A_F, A_S, A_R, A_C] \tag{3}$$

The resultant augmented image A_{AU} obtained during augmentation of segmented image T_S is applied to different feature extractors for the extraction of relevant features.

5) Feature extraction

The most relevant features suitable for the classification of leukemia are obtained during the process of feature extraction. Here, features such asGLCM features, statistical features, CLBP, PHOG, LVP, LGXP, and CNN features are extracted. The extraction processes performed are explicated in this section.

i) Statistical features

The various statistical features, namely mean, median, kurtosis, skewness, variance, and standard deviation [23] are extracted using different extractors and the processes carried out during extraction are enumerated below,

-***Mean:*** It is termed as the data concentration of a distribution and is computed using the expression designated as,

$$M_1 = \sum_{d=1}^{l-1} \left(B(d)\right) \tag{4}$$

here, l represents total number of grey levels, the image grey scale level is indicated as d ,the probability of d is denoted as $B(d)$, and M_1 signifies extracted mean feature.

-***Median:*** The median is considered a numerical value that is used to split the probability distribution into equal parts. The chances of leukemia abnormality are higher when a high

difference among the median is determined. Similarly, the higher the chances of no anomalies results in small differences among the median. Therefore, the extracted median feature is represented by the term M_2.

-Standard deviation: The data dispersion near the mean is defined as standard deviation and is computed using the expression,

$$M_3 = \sqrt{\sum_{d=1}^{l-1}(d - M_1)^2 * B(d)} \tag{5}$$

here, the extracted standard deviation feature is represented as M_3.

-Variance: The variance feature is used to indicate deviation value of image grey levels corresponding to mean grey level. The expression used to determine variance feature is expressed by,

$$M_4 = \sum_{d=1}^{l-1}(d - M_1)^2 * B(d) \tag{6}$$

where, M_4 indicates the extracted variance feature.

-Skewness: The asymmetrical distributed degree of features around the mean is termed skewness and is expressed as,

$$M_5 = M_1^{-3}\left[\sum_{d=1}^{l-1}(d - M_1)^3 * B(d)\right] \tag{7}$$

where the extracted skewness feature is represented as M_5.

-Kurtosis: In general, kurtosis is termed as a fourth normalized moment utilized to determine the normal distribution leveling. The kurtosis is determined by the expression designated as,

$$M_6 = \mathrm{M}_1^{-4}\left[\sum_{d=1}^{l-1}(d - M_1)^4 * B(d)\right] \tag{8}$$

here, the extracted kurtosis feature is signified as M_6.

ii) GLCM features

The GLCM feature [11] is used to effectively characterize the image textures for the extraction of statistical texture parameters. Here, the GLCM features, like entropy, contrast, correlation, energy, and homogeneity are extracted from the augmented blood smear image A_{AU}. The process carried outis briefly enumerated below,

-Contrast: It is utilized to estimatethe spatial frequency of image and helps to determine various GLCM moments. Generally, the contrast is the variation among the adjacent highest and lowest pixel sets, where the contrast is estimated by,

$$\mathrm{M}_7 = \sum_{\mathrm{U}=0}^{\mathrm{l}-1} \sum_{\mathrm{V}=0}^{\mathrm{l}-1} \mathrm{K}(\mathrm{U}-\mathrm{V})^2 \tag{9}$$

here, the extracted contrast feature is represented as M_7, and $\mathrm{K}(\mathrm{U},\mathrm{V})$ signifies the normalized value of gray-scale at kernel positions U and V.

-Correlation: It is used to estimate the occurrence of joint probability of specified pairs of pixels, and is determined using the expression given by,

$$\mathrm{M}_8 = \sum_{\mathrm{U}=0}^{\mathrm{l}-1} \sum_{\mathrm{V}=0}^{\mathrm{l}-1} \frac{(\mathrm{U}\times\mathrm{V})\times\mathrm{K}(\mathrm{U},\mathrm{V}) - (\chi_a \times \chi_b)}{(\delta_a \times \delta_b)} \tag{9}$$

where, M_8 denotes the extracted correlation feature, χ signifies mean, and the standard deviation is indicated as δ.

-Energy: The Square of the angular second moment is used to determine energy and is given by the expression,

$$M_9 = \sqrt{\sum_{\mathrm{U}=0}^{\mathrm{l}-1} \sum_{\mathrm{V}=0}^{\mathrm{l}-1} \mathrm{K}(\mathrm{U},\mathrm{V})^2} \tag{10}$$

here, M_9 indicates the energy feature.

-Homogeneity: The homogeneity helps to estimate the approximation of distribution of elements. The homogeneity is evaluated using the formula given by,

$$M_{10} = \sum_{\mathrm{U}=0}^{\mathrm{l}-1} \sum_{\mathrm{V}=0}^{\mathrm{l}-1} \frac{\mathrm{K}(\mathrm{U},\mathrm{V})}{1+(\mathrm{U}+\mathrm{V})^2} \tag{11}$$

where, M_{10} denotes the extracted homogeneity feature.

-Entropy: It is used to determine large pixel information as well as information of corner and edge pixels. The entropy feature is given by the expression,

$$M_{11} = -\sum_{U=0}^{l-1}\sum_{V=0}^{l-1} \mathrm{K(U,V)} \times \log\left(\mathrm{K(U,V)}\right) \tag{12}$$

here, the entropy feature extracted from the augmented blood smear image A_{AU} is given as M_{11}.

iii) CLBP: The local information from the augmented blood smear image A_{AU} is extracted using the CLBP feature [12]. It is utilized to increase the robustness of textural feature representation and characterize discriminate information from the image. The CLBP effectively addressed different background interference issues that arise due to grayscale invariance. It helps to code the local region by using a central pixel, where the expression of CLBP is given by,

$$M_{12} = \sum_{f=0}^{f-1} \mu(D_f - O)2^f \tag{13}$$

where, f indicates the neighborhood pixel, O denotes mean value, D_f is the magnitude component, the gray value of central pixel is represented as O, sign component is represented as μ, and M_{12} is used to represent the CLBP feature extracted from augmented blood smear image A_{AU}.

iv) PHOG: The PHOG [13] acts asa spatial shape descriptor, which is used to indicate the spatial distribution of edges. The PHOG is designed by considering Histogram of Oriented Gradients (HOG) and also theuse of pyramid representation. The images are distributed over edge orientation inside the region and tiltedat different resolutions into the regions. At each resolution, the HOG is presented in the sub-region of each image. The PHOG feature is extracted by initially extracting edge contours and the images are split into cells at different

pyramid levels. Then, the HOG of grids of each pyramid resolution level is evaluated and the image PHOG descriptor is finally concatenated with HOG vectors at each pyramid resolution. Thus, the final extracted PHOG feature is indicated as M_{13}.

v) LGXP: The various phases of LGXP is initially quantized to various range and the Local XOR Pattern (LXP) operator [15] is used to perform quantization of central pixel as well as its neighbors. The concatenation is performed on the resultant binary labels with the local pattern of central pixel and the expression of the LGXP pattern under the decimal and binary form is given by,

$$M_{14} = \left[N_{e,d}^{g}, N_{e,d}^{g-1}, ..., N_{e,d}^{1}\right]_{binary} = \left[\sum_{X=1}^{g} 2^{X-1}.N_{e,d}^{X}\right]_{decimal} \tag{14}$$

where, $N_{e,d}^{g}(X = 1,2,3,....,g)$ denotes the estimated pattern, e denotes the orientation, g represents the neighbourhood size o, the scale is represented as d, and the extracted LGXP feature is represented as M_{14}.

vi) CNN: The CNN [24] are deep and feed-forward artificial neural network, which possesses three layers, namely convolutional, fully connected, and pooling layer. The diverse input features are extracted using a convolutional layer. Generally, the over-fitting issues, computational cost, and total number of parameters are reduced using the pooling layer. Moreover, fully connected layer is utilized to incorporate features with the preceding convolutional layer. The share weights and local connectivity are utilized by CNN to increase efficiency, the feature produced by the conv layer is defined as the CNN feature and is represented as M_{15} and the structure of the CNN feature is portrayed in figure 2.

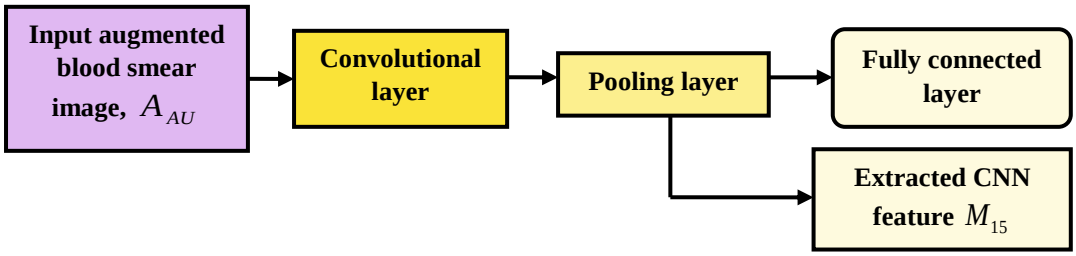

Figure 2. Structureof CNN feature

vii) LVP: The LVP feature [14] is used to compute the targeted and adjacent pixels from various directions using diverse distancesto identify the structure information of local textures as well as one-dimensional direction. In LVP, the pair-wise orientation vectors are encoded for the extraction of micropatterns isperformed using Comparative Space Transform (CST). The length and redundancy of data features are effectively reduced using the LVP feature and M_{16} signifies extracted LVP feature, which is expressed as,

$$M_{16} = LVP_{x,y}(\varepsilon) = \left\{ LVP_{x,y,\phi}(\varepsilon) \mid \varepsilon = 0^{o}, 45^{o}, 90^{o}, 135^{o} \right\} \tag{15}$$

here, the extracted LVP feature is represented as M_{16}, the reference pixel is given by ε, the radius of the neighborhood is symbolized as y, ϕ signifies vector direction, and x indicates total neighborhood pixel.

Thus, the extracted statistical, GLCM, CLBP, PHOG, LVP, LGXP, and CNN features are finally designated as,

$$M = \left[M_1, M_2, M_3, ..., M_{16} \right] \tag{16}$$

The resultant extracted feature M obtained during feature extractionis further fed into TSCO-L-LeNet for the classification of leukemia.

6) Leukemia classification using TSCO- L-LeNet model

Leukemia occurs due to the excess creation of abnormal or immature leukocytes. Leukemia is classified by determining the chronic and acute progress of the disease and also by considering the affected rate of white blood cells. Here, the classification of leukemia is performed using the L-LeNet-TSCO model. The deep learning models, LeNet [16] and LSTM [17] are integrated to introduce the L-LeNet model for leukemia classification. The optimal weights of L-LeNet are fine-tunedby using TSCO algorithmic technique. The TSCO is designed by the incorporation of TSA [18] and SCSO [19] algorithmic approaches. Thus, the process of leukemia classification using TSCO-L-LeNet is briefly demonstrated below,

I. Designed L-LeNet for leukemia classification

In general, immediate treatment and prognosis of patients with leukemia disease is provided by early classification of leukemia. The L-LeNet model designed in this research is used to accurately classify leukemia as chronic or acute. The L-LeNet is designed by integrating deep learning models, like LeNet [16] and LSTM [17]. The leukemia classification process is performed using three components, like LeNet model, the L-LeNet layer, and the LSTM model. Moreover, the regression modeling is performed in the L-LeNet layer using Fractional Calculus (FC) [25] for the fusion of LeNet and LSTM by increasing the strength of the fusion task. During the process of leukemia classification, the input blood smear image taken for leukemia classification W_E is initially fed into the LeNet model to obtain the output R_1. The output R_1 obtained from L-LeNet model and the features extracted M are applied to L-LeNet layer for fusion to obtain output R_2. Finally, the output R_2 is fed into LSTM model to obtain the final classified leukemia output R_3. In addition, the modeling of the L-LeNet model for the classification of leukemia is given in figure 3.

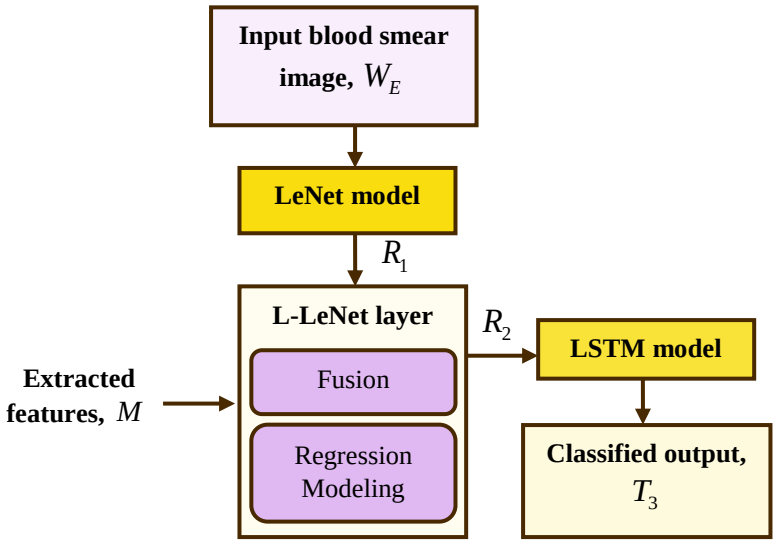

Figure 3. Schematic representation of L-LeNet model for leukemia classification

a) LeNet model

The LeNet [16] is a CNN structure with gradient-based learning, where the input blood smear image taken for leukemia classification W_E is fed into input layer and obtains output from output layer. The LeNet model is small and straight forward, which comprises deep layers that help to classify disease more accurately under less training time. It also comprises one fully connected, two pooling, and three convolutional layers. The fully connected layer in the LeNet helps to reduce total training parameters and neurons. The processes performed in each layer are enumerated below,

a) Convolutional layer: The process of feature extraction is mainly performed in convolutional layer. In general, convolutional kernels are generally presented in each convolutional layer, where the convolutional layer is expressed as,

$$C_{m,n} = \left[f\left(\sum_{i=0}^{g-1} \sum_{j=0}^{g-1} X_{i,j} r_{m+i,n+j} + s \right) \right]_{m=1,2,...E;n=1,2,..,F} \tag{17}$$

here, $f(\bullet)$ denotes activation function, the convolutional output is indicated as $C_{m,n}$, $r_{m,n}$ denotes input matrix, the convolution kernel is given by $X_{i,j}$, the convolution offset term is signified as s, the size of convolutional kernel is represented as g, and the size of input matrix is symbolized as E and F.

b) Activation function: The LeNet uses the five most commonly utilized activation functions, like Rectified Linear Unit (ReLu). The saturating nonlinear functions, like Gaussian, Sigmoid, and Tanh are widely used activation functions in classical CNN, which is given by the expression,

$$f(r) = \frac{1}{1+e^{-r}} \tag{18}$$

$$f(r) = \frac{e^{r} - e^{-r}}{e^{r} + e^{-r}} \tag{19}$$

$$f(r) = e^{-r^2} \tag{20}$$

At present, the unsaturated nonlinear functions Softplus and ReLu are also utilized in CNN structures as activation functions and are expressed as,

$$f(r) = \max(0.r) \tag{21}$$

$$f(r) = \ln(1 + e^{r}) \tag{22}$$

From the expression, the unsaturated nonlinear functions are used to provide solutions to the disappearance of gradient as well as gradient explosion issues. It also increases the CNN performance as well as convergence speed during classification. Moreover, the ReLU functions are faster than the saturating nonlinear function and when the input is positive it doesn't have any gradient saturation issue.

c) Pooling layer: The dimension of data is reduced by pooling layer via feature selection process during conserving main data characteristics. In the LeNet structure, the input feature matrix is decreased into two dimensions and the pooling operation performed is designated as,

$$C_j^k = pool\left(C_j^{k-1}\right) \tag{23}$$

here, C_j^k indicates the output of k^{th} layer, the corresponding j^{th} sample is represented as j , and the preceding layer output is signified as C_j^{k-1}

d) Fully connected layer: The fully connected layer is the final layer of the CNN structure where ReLU activation function is utilized by each neuron to fully link the neurons to the previous layer. Moreover, the local information is integrated by fully connected layer and the resultant output is passed to output layer. Thus, the fully connected layer perform the tasks played by conventional classifiers and the output obtained by fully connected layer is given by,

$$C_j^k = f\left(X^k . C_j^{k-1} + s^k\right) \tag{24}$$

here, the convolutional kernel is indicated as X^k, and the offset term is represented as s^k.

e) Softmax layer: It is the output layer of the LeNet model, and is highly utilized for multiple classification processes, where the softmax layer maps the output of fully connected layer to a probability (0,1). At last, the output is chosen by taking maximum probability, which is designated as,

$$C_j^K = R_1 = Soft\max\left(X^K . C_j^{K-1} + s^K\right) \tag{25}$$

where, R_1 denotes the output of LeNet model, and K represents the final softmax layer. The final output LeNet model R_1 is sent to the L-LeNet layer and figure 4 depicts the structure of LeNet model.

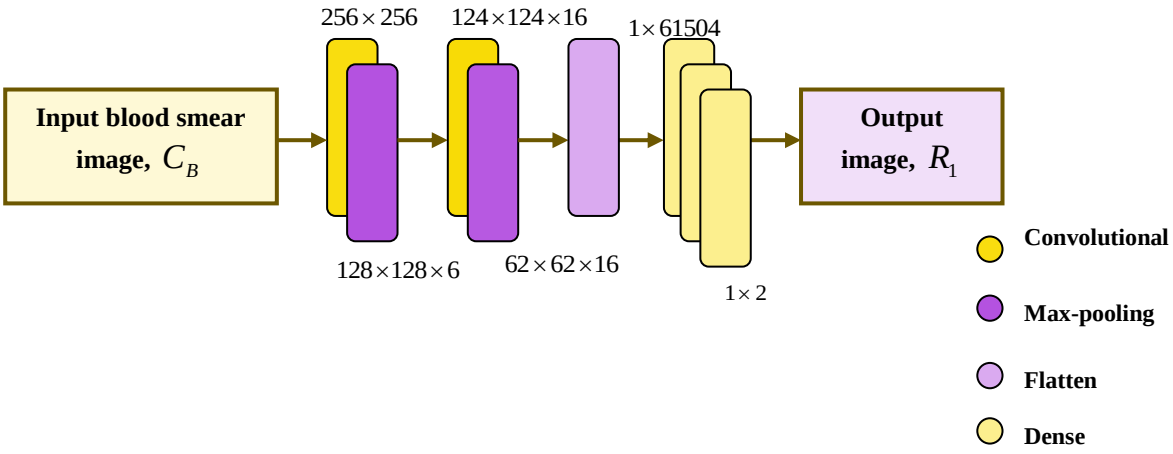

Figure 4. Architecture of LeNet model

b) L-LeNet layer

In the L-LeNet layer, the output of the LeNet model R_1 and extracted features M are passed for the fusion of LeNet [16] and LSTM [17] models. The regression modeling is executed to accomplish the fusion process by identifying the relationship between the inputs. Here, the FC [25] is used to perform regression modeling, where FC uses the Laplace transform for providing solutions to various integral as well as derivative equations, and the original results are obtained by executing inverse operations. The output of the L-LeNet layer is determined

by taking account of weighted features. At different time intervals, the output obtained by the L-LeNet layer is explicated below.

Therefore, at g^{th} time intervals the output obtained by the L-LeNet layer is designated as,

$$\psi = \sum_{e=1}^{t} M_{SG_e} * Q_e \tag{26}$$

where, Q indicates weight coefficient, the extracted statistical and GLCM feature is denoted as M_{SG} and is given by $M_{SG} = [M_1, M_2, M_3, ..., M_{11}]$, and t denotes number of images. The L-LeNet layer output at $(g-1)^{th}$ interval is given by,

$$\psi_1 = \sum_{e=1}^{t} \sum_{f=1}^{S} M_{12_{ef}}^{2} * Q_{ef} \tag{27}$$

here, M_{12} indicates the CLBP feature extracted from the augmented blood smear image A_{AU}. In addition, at $(g-2)^{th}$ intervals, the output recorded by the L-LeNet layer is given by,

$$\psi_2 = \sum_{e=1}^{t} \sum_{f=1}^{S} M_{13_{ef}}^{2} * Q_{ef} \tag{28}$$

where, the PHOG feature extracted is symbolized as M_{13}, and the L-LeNet layer output at interval $(g-3)$ is expressed as,

$$\psi_3 = \sum_{e=1}^{t} \sum_{f=1}^{S} M_{16_{ef}}^{2} * Q_{ef} \tag{29}$$

The term M_{16} signifies the LVP feature extracted from the augmented blood smear image A_{AU}. Moreover, the L-LeNet layer output at $(g-4)^{th}$ interval is expressed as,

$$\psi_4 = \sum_{e=1}^{t} \sum_{f=1}^{S} M_{14_{ef}}^{2} * Q_{ef} \tag{30}$$

where, the LGXP feature extracted is depicted as M_{14}, and L-LeNet layer output at $(g-5)^{th}$ interval is expressed as,

$$\psi_5 = \sum_{e=1}^{t}\sum_{f=1}^{S} M_{15_{ef}}^2 * Q_{ef} \tag{31}$$

where, M_{15} is indicated as the CNN features extracted using the CNN feature extractor. The FC [25] is employed for the fusion of the LeNet [16] and LSTM [17] models via regression modeling. Hence, from FC,

$$\begin{aligned} R_2 = Y\cdot\psi + \frac{1}{2}Y\cdot\psi_1 + \frac{1}{6}(1-Y).\psi_2 + \frac{1}{24}Y(1-Y)(2-Y)\cdot\psi_3 + \frac{1}{120}Y(1-Y)(2-Y)(3-Y)\cdot\psi_4 \\ + \frac{1}{720}Y(1-Y)(2-Y)(3-Y)(4-Y)\cdot\psi_5 + \frac{1}{5040}Y(1-Y)(2-Y)(3-Y)(4-Y)(5-Y)\cdot R_1 \end{aligned} \tag{32}$$

By substituting the value of $\psi, \psi_1, \psi_2, \psi_3, \psi_4,$ and ψ_5, the final output of the L-LeNet layer is designated as,

$$\begin{aligned} R_2 = Y\cdot\left[\sum_{e=1}^{t} M_{SG_e} * Q_e\right] + \frac{1}{2}Y\cdot\left[\sum_{e=1}^{t}\sum_{f=1}^{S} M_{12_{ef}}^2 * Q_{ef}\right] + \frac{1}{6}(1-Y).\left[\sum_{e=1}^{t}\sum_{f=1}^{S} M_{13_{ef}}^2 * Q_{ef}\right] \\ + \frac{1}{24}Y(1-Y)(2-Y)\cdot\left[\sum_{e=1}^{t}\sum_{f=1}^{S} M_{16_{ef}}^2 * Q_{ef}\right] + \frac{1}{120}Y(1-Y)(2-Y)(3-Y)\cdot\left[\sum_{e=1}^{t}\sum_{f=1}^{S} M_{14_{ef}}^2 * Q_{ef}\right] \\ + \frac{1}{720}Y(1-Y)(2-Y)(3-Y)(4-Y)\cdot\left[\sum_{e=1}^{t}\sum_{f=1}^{S} M_{15_{ef}}^2 * Q_{ef}\right] \\ + \frac{1}{5040}Y(1-Y)(2-Y)(3-Y)(4-Y)(5-Y)\cdot R_1 \end{aligned} \tag{33}$$

where, the order of derivative is represented as Y and the output R_2 recorded by L-LeNet layer is further sent for further leukemia classification using LSTM model.

c) LSTM model

The LSTM [17] model is the variant of the Recurrent Neural Network (RNN), which is used to indicate the long-term dependency of time series data. The LSTM is used to provide a solution to vanishing gradient issues in certain cases during memorization of long-term

context is necessary. The constant error flows are regulated using nonlinear units by learning to close or open the network gates. The LSTM expedites conventional RNN algorithms by approximating the long-term information with necessary delays. The cell state, which is more similar to the conveyor belt is the major key of LSTM. The optional inlet of information is created by using gates, where the gate comprises a point wise multiplication operation and a sigmoid neural net layer. The hidden state of the LSTM model is determined using the expression enumerated as follows,

Initially, the information considered is taken from cell state is decided by considering forget gate, which is expressed as,

$$S_f = \xi\left(R_{2f} Z^a + G_{f-1} H^a + \varepsilon_a\right) \tag{34}$$

here, R_2 represents the input time step, G_{f-1} indicates previous time step hidden state. In the cell state, the new information is stored using two folds, namely the input layer and the tanh layer. The values to be modified are decided in the input gate layer and a new candidate vector value is created in the tanh layer. The process performed is designated as,

$$c_f = \xi\left(R_{2f} Z^c + G_{f-1} H^c + \varepsilon_c\right) \tag{35}$$

$$\tilde{I}_f = \tanh\left(R_{2f} Z^I + G_{f-1} H^I + \varepsilon_I\right) \tag{36}$$

Afterward, the old cell state I_{f-1} is modified into a new cell state I_f, and is expressed as,

$$I_f = I_{f-1} \otimes S_f \oplus c_f \otimes \tilde{I}_f \tag{37}$$

Finally, the output is obtained in the filtered version by considering the cell state through the output gate. Here, the parts of cell state are decided by cell gate to produce output and pass the cell state via the tanh layer, it also multiplies the output gate using the expression given below,

$$R_3 = \xi\left(R_{2f} Z^{R_3} + G_{f-1} H^{R_3} + \varepsilon_{R_3}\right) \tag{38}$$

where, Z^a, Z^c, Z^I, and Z^{R_3} signifies the input weight, and the bias is denoted as $\varepsilon_a, \varepsilon_c, \varepsilon_I$, and ε_{R_3}. Also, the recurrent weights are represented as H^a, H^c, H^I, and H^{R_3}. The output R_3 obtained from the LSTM model is the final leukemia classified output and the structure of LSTM is displayed in figure 5.

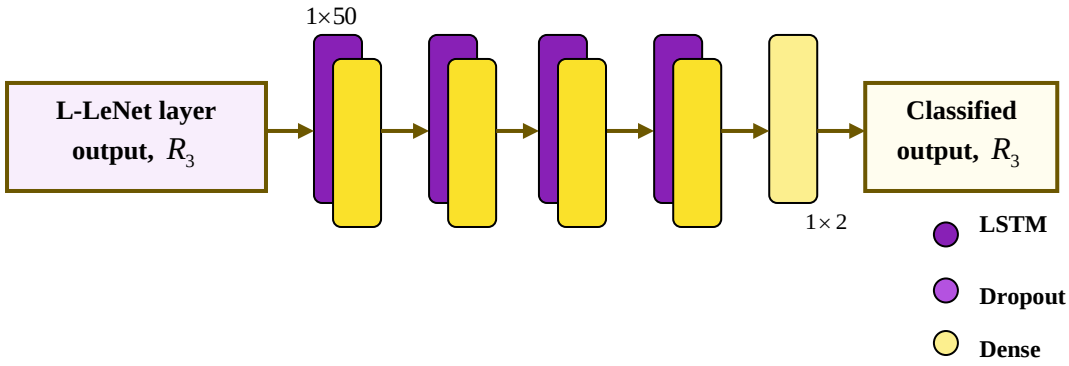

Figure 5. Structure of LSTM model

II. TSCO model for tuning L-LeNet

The performance of the L-LeNet used for the classification of leukemia is increased by fine-tuning the optimal weights of the L-LeNet using the TSCO algorithmic approach. The TSCO is designed by the incorporation of TSA [18] and SCSO [19] approaches. The SCSO is designed by considering the identifying ability to sense fewer frequency noises by the sand cat. The transitions of exploitation and exploration phase are effectively balanced by SCSO model. It also determine optimal solutions by utilizing few parameters. Moreover, TSA is designed by considering tangent function for moving the solution towards an optimal solution. The TSA approach effectively balance the search space among exploration and exploitation phase, which also comprises good convergence capacity. The integration of TSA with SCSO is performed to obtain user-defined parameters as well as it also increase the classification performance. The modified equation of TSCO is designated as,

$$h(p+1)=\frac{1}{1+step*\tan\theta+m.R(0,1)}\left[m\left(h_{best}(p)(1+)step*\tan\theta-R(0,1).step*\tan\theta*y_{opt}(p)\right)\right] \tag{39}$$

where, $h(p+1)$ represents the position of solution at $(p+1)$iteration, R signifies random number, which is fixed to $[0,1]$, the movement size of step is signified as $step$, and the sensitivity range of cat is symbolized as m. The fitness value is considered for the determination of optimal solution, which is estimated using Mean Square Error (MSE) and is expressed as,

$$FF=\frac{1}{F}\sum_{\phi=1}^{F}\left(R_{3\phi}^{*}-R_{3\phi}\right)^{2} \tag{40}$$

here, the total samples are represented as F, R_3^* indicates the targeted L-LeNet output, and R_3 denotes the original output of L-LeNet.

7) Incremental learning for leukemia classification

The incremental learning is used to provide solutions to various issues that occur in L-LeNet while classifying leukemia that are not provided initially in the database. It is generally applied in certain cases where the storage of all data is not feasible and the input is obtained in sequential order. It effectively assesses the confusable classes that cause the performance of the L-LeNet model used for leukemia classification. Let us consider incremental data J^{l+1} and also, consider the error by the L-LeNet during leukemia classification be e^{l+1}, where time is represented as l. The weights are bounded based on holo-entropy if the error $e^{l+1}>e^{l}$ or else, no training is performed. The holo-entropy is used to estimate the unpredictability of content information and the targeted value of the information presented in the classified image. The informative contents are measured easily by using holoentropy [26], thus making the classification process simpler. Here, the modified weights are based on the bounded weights of L-LeNet and are expressed as,

$$k^{l+1} = k^{l} \pm k^{\eta} \tag{41}$$

here, the weights are symbolized as k, the holo-entropy based on the weight coefficient is signified as k^{η}. The holo-entropy decision is performed initially by building a decision tree and the holo-entropy is estimated for every feature attribute by using the expression given by,

$$\gamma = k.\vartheta(d_x) \tag{42}$$

$$k = 2\left(1 - \frac{1}{1 + \exp(-\vartheta(d_x))}\right) \tag{43}$$

$$\vartheta = \sum_{x=1}^{\rho} E_x \log E_x \tag{44}$$

where, the attribute vector is represented as d_x, the total unique values presented in the attribute vector is indicated as ρ, and γ denotes holoentropy.

4. Results and discussion

The leukemia classification performance of TSCO-L-LeNet is identified by comparing the results obtained from the experiment with existing leukemia classification techniques and the discussion followed is enumerated below,

4.1. Experimental set-up

The Python tool is used for the implementation of TSCO-L-LeNet model for the classification of leukemia using blood smear images.

4.2. Dataset description

The Blood Cells Cancer (ALL) dataset [20] is used to diagnose ALL by utilizing peripheral blood smear images, which includes screening of cancer cases initially from non-cancer cases. The database comprises 3242 blood smear images collected from 89 patients who are

suspicious of ALL in bone marrow laboratory of Taleqani Hospital. High-skilled laboratory staffs are used to prepare and stain the blood samples and the images are categorized into malignant and benign classes. The malignant lymphoblasts of the ALL group are categorized into three sub-types, namely Pro-B ALL, Pre-B, and Early Pre-B. The images presented in the database are in Joint Photographic Experts Group (JPG) file form, which are taken using a Zeiss camera in a microscope with a 100x magnification.

4.3. Evaluation paramters

The superiority of TSCO-L-LeNet during leukemia classification is identified by utilizing various evaluation parameters and is enumerated below,

a) Accuracy: It is the relationship between the original and targeted output acquired by TSCO-L-LeNet while classifying leukemia and is formulated as,

$$Accuracy = \frac{L_{TP} + L_{TN}}{L_{TP} + L_{TN} + L_{FP} + L_{FN}} \tag{45}$$

here, L_{TP} and L_{TN} signifies true positive and true negative, false positive and false negative are represented as L_{FP} and L_{FN}.

b) TPR: TPR is the ratio of the precisely classified positive samples from input total positive samples and is expressed as,

$$TPR = \frac{L_{TP}}{L_{TP} + L_{FN}} \tag{46}$$

c) TNR: TNR is the proportion of precisely classified negative samples from input total negative samples and is designated as,

$$TNR = \frac{L_{TN}}{L_{TN} + L_{FP}} \tag{47}$$

4.4. Image results

The outcomes recorded during leukemia classification using the TSCO-L-LeNet model are displayed in Figure 6. Figure 6(a), 6(b), and 6(c) show the input, pre-processed, and segmented image results. Moreover, figure 6(d) elucidates the extracted CLBP image and LGXP images are given in figure 6(e).

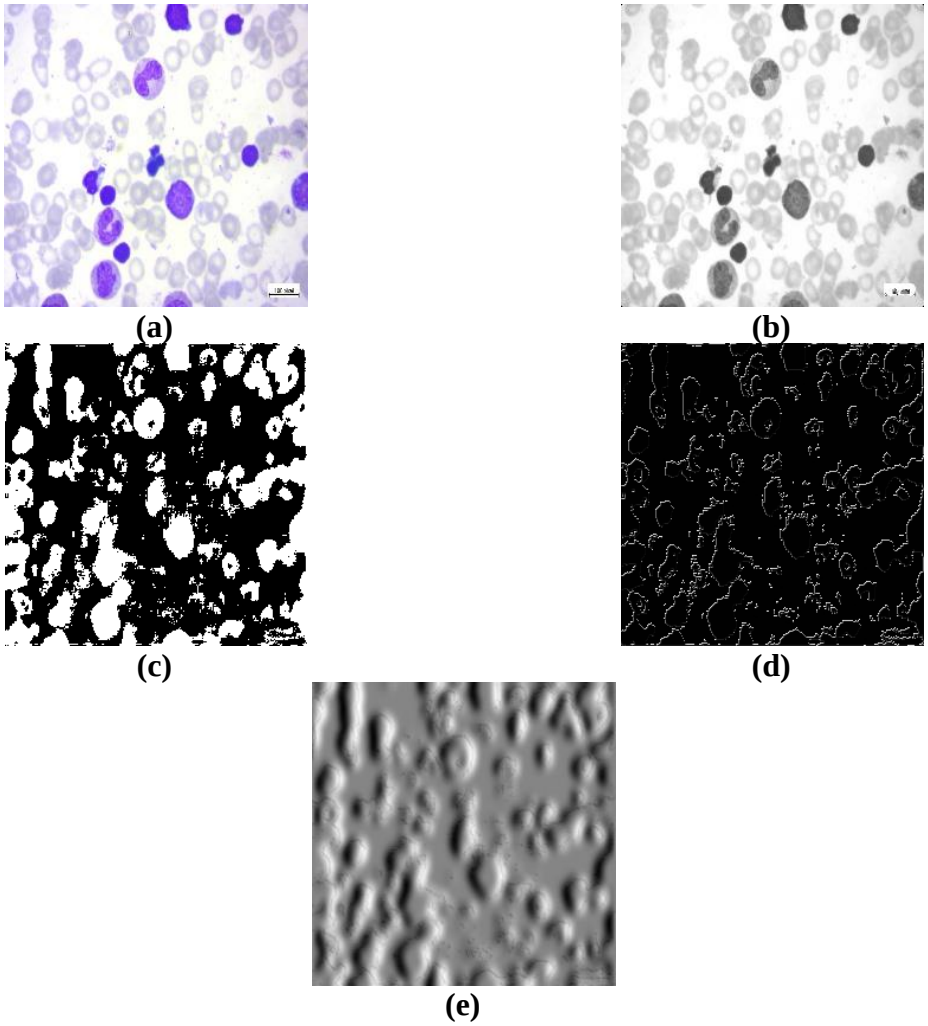

Figure 6. Experimental image results of TSCO-L-LeNet (a) Input, (b) pre-processed (c) segmented, (d) CLBP, and (e) LGXP feature

4.5. Performance analysis

The K-fold value as well as the percentage training set is varied to analyze the superiority of TSCO-L-LeNet during the classification of leukemia.

- Analysis using training set

The analysis of performance of TSCO-L-LeNet used for the classification of leukemia is depicted in figure 7. The evaluation of TSCO-L-LeNet utilizing TPR is given in figure 7(a), where the TPRof0.821, 0.862, 0.882, and 0.932 is recorded by TSCO-L-LeNet for training set of 80% for epochs 10, 20, 30, and 40. In figure 7(b), the evaluation of TSCO-L-LeNet using TNRis displayed. The TSCO-L-LeNet measured TNR of 0.866, 0.883, 0.896, and 0.942 for epochs of 10, 20, 30, and 40 for 80% training set. Moreover, in figure 7(c) the performance of TSCO-L-LeNet employing accuracy is elucidated. The TSCO-L-LeNet model measured0.841, 0.861, 0.896, and 0.923 accuracy for training set of 80% and for epochs of 10, 20, 30, and 40.

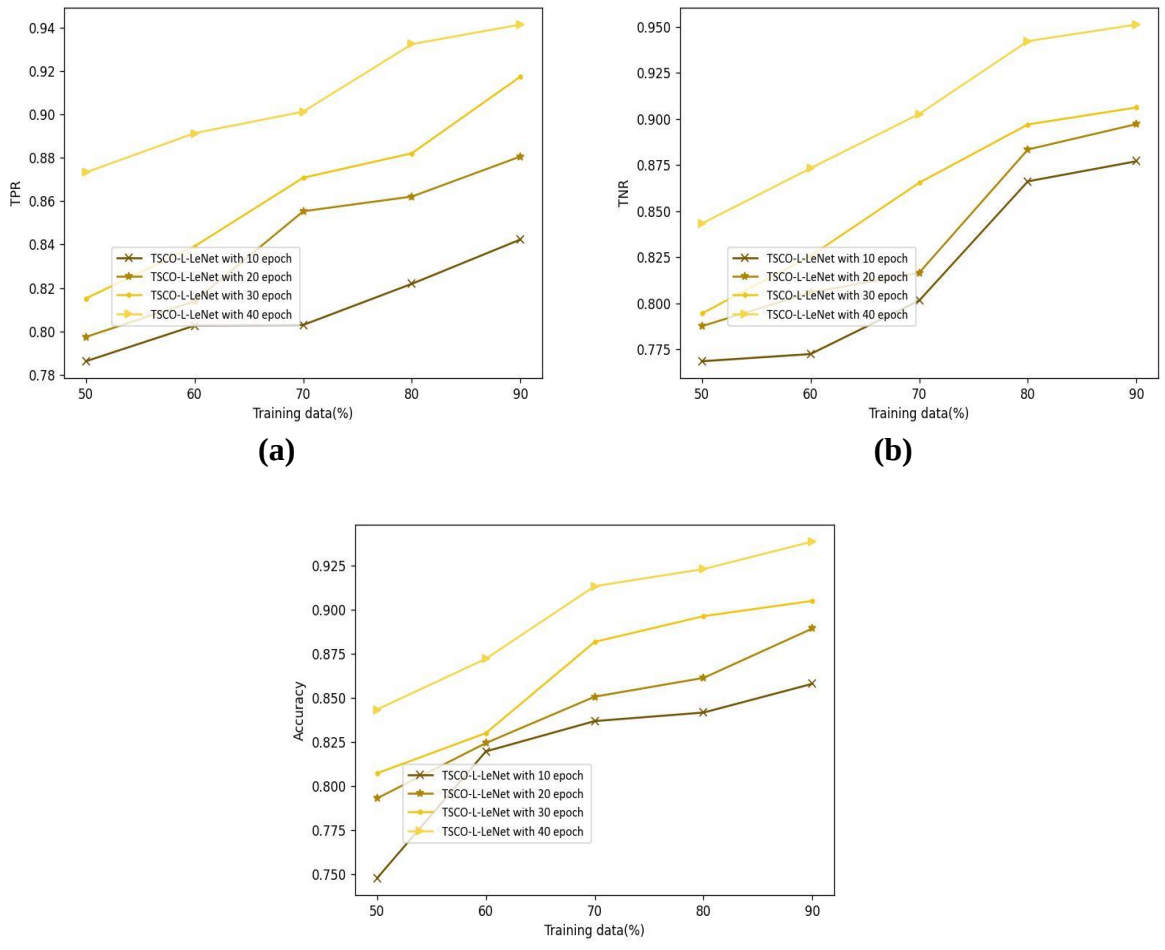

Figure 7. Performance evaluation of TSCO-L-LeNet utilizing training set(a) TPR, (b) TNR, and (c) Accuracy

-Analysis using K-fold value

Figure 8 illustrates the evaluation of TSCO-L-LeNet utilized for leukemia classification. The analysis performed by utilizing TPR is shown in figure 8(a), where the TSCO-L-LeNet model recorded TPR of 0.823, 0.837, 0.891, and 0.925 for epochs of 10, 20, 30, and 40 for K-fold value of 8. The performance analysis using TNR of TSCO-L-LeNet is shown in figure 8(b).The TNR of 0.843, 0.868, 0.901, and 0.933 is measured by TSCO-L-LeNet for epoch of 10, 20, 30, and 40 for K-fold value 8. Moreover, figure 8(c) depicts the analysis performed by utilizing accuracy, where TSCO-L-LeNet gained accuracy for K-fold value 8 is 0.857, 0.862, 0.881, and 0.926for epochs 10, 20, 30, and 40.

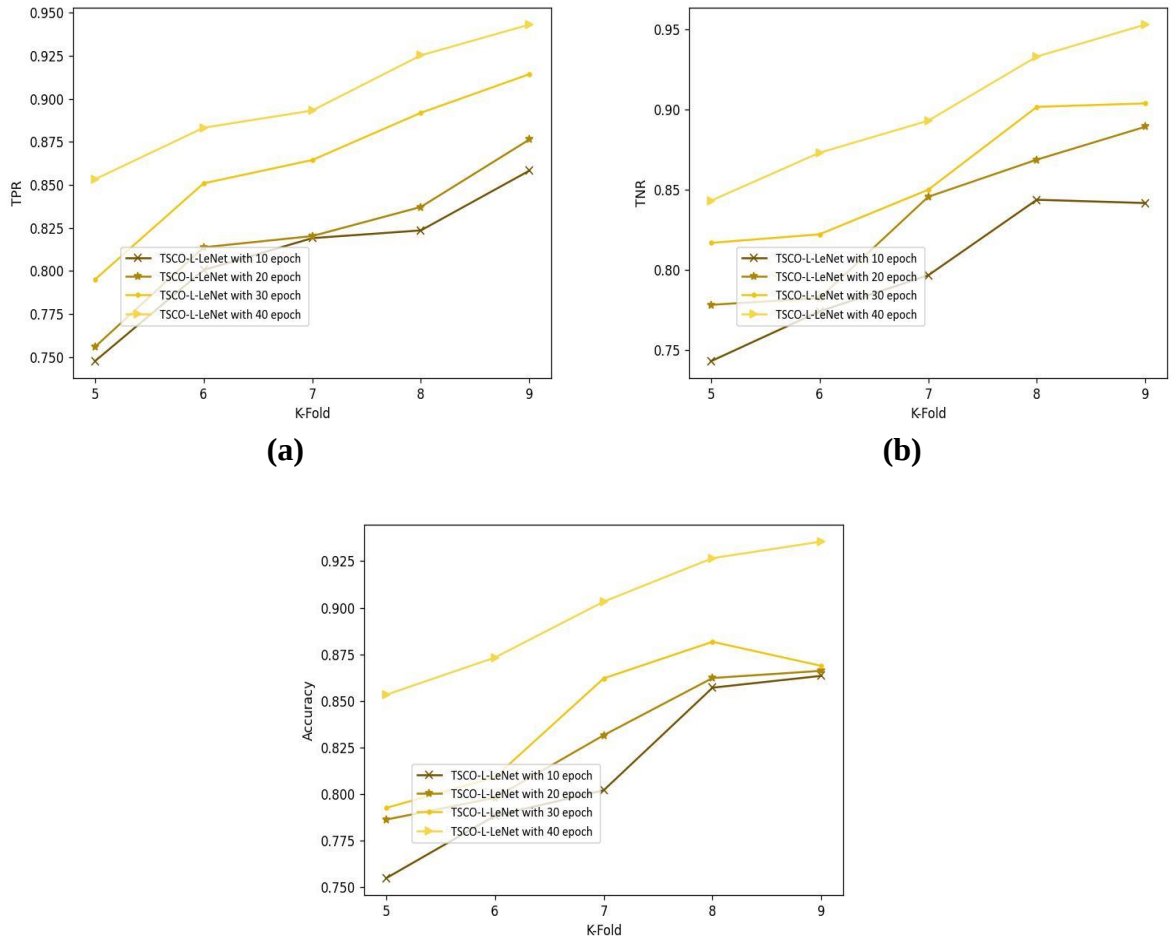

Figure 8. Performance evaluation of TSCO-L-LeNet using K-fold ((a) TPR, (b) TNR, and (c) Accuracy

4.6. Comparative models

The leukemia classification performance of TSCO-L-LeNet is determined by comparing the performance of TSCO-L-LeNet with other existing classification approaches. The existing models, like Enhanced incremental training [1], Inception v3 XGBoost [2], ResR and SVM [3], and ECA-VGG16 [4] are considered for comparison.

4.7. Comparative analysis

The superiority of TSCO-L-LeNet is determined by varying value of K-fold and training set percentage, where the analysis performed is demonstrated below,

- Analysis using training set

The leukemia classification performance of TSCO-L-LeNet is analysed by utilizing a training set is elucidated in figure 9. The evaluation using TPR of different approaches is shown in figure 9(a). The TSCO-L-LeNet gainedTPRof0.922for 80% training set and the existing classification approaches, namely Enhanced incremental training, Inception v3 XGBoost, ResRandSVM, and ECA-VGG16 measured TPR of 0.834, 0.836, 0.849, and 0.851. It is proven that TSCO-L-LeNet achieved high performance of 7.89% as compared with existing ResRandSVM classification technique. Figure 9(b) depicts valuation of the performance of leukemia classification models using TNR. The TNR measured by the models for the training set of 80% is 0.816 by Enhanced incremental training, 0.838 by Inception v3 XGBoost, 0.842 by ResRandSVM, 0.857 by ECA-VGG16, and 0.914by TSCO-L-LeNet. Here, the TSCO-L-LeNet attained high performance of 8.32% as compared with Inception v3 XGBoost. The analysis utilizing accuracy of different classification techniques is given in figure 9(c). The TSCO-L-LeNet measured accuracy of 0.926for 80% training set. Likewise, accuracy obtained by other existing approaches, such as Enhanced incremental training is 0.836, Inception v3 XGBoost is 0.871, ResRandSVM is 0.885, and ECA-VGG16 is 0.887. The

analysis proved that the TSCO-L-LeNet achieved a maximum accuracy of 4.23% than the ECA-VGG16 scheme.

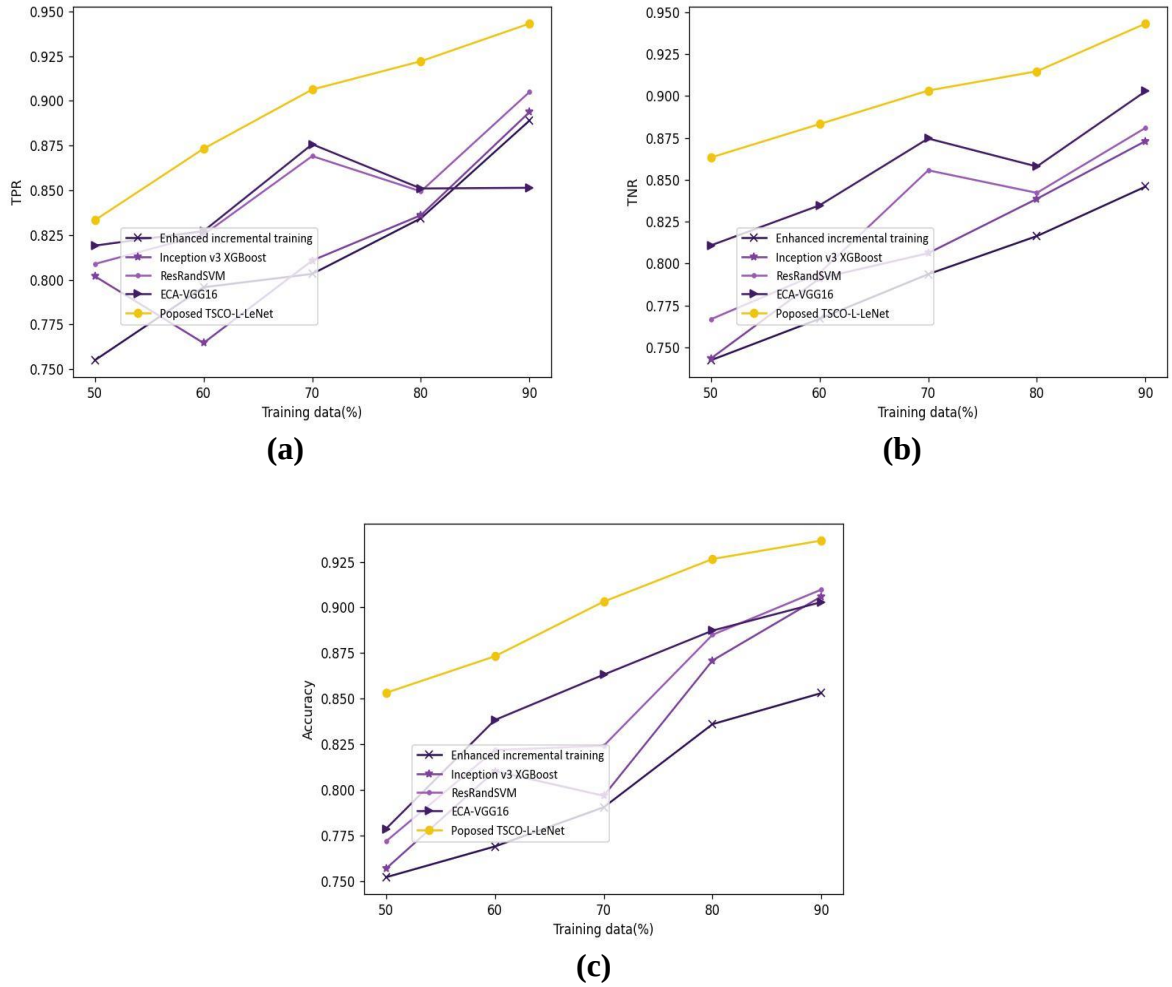

Figure 9. Comparative evaluation of TSCO-L-LeNet utilizing training set ((a) TPR, (b) TNR, and (c) Accuracy

-Evaluation using K-fold value

The evaluation of TSCO-L-LeNet utilized for leukemia classification using K-fold is elucidated in figure 10. Figure 10(a) shows analysis using TPR of leukemia classification models. The TPR gained by the leukemia classification models is 0.915 by Enhanced incremental training, 0.841 by Inception v3 XGBoost, 0.857 by ResRandSVM, 0.871 by ECA-VGG16, and 0.829 by TSCO-L-LeNet for K-fold value 8. The TSCO-L-LeNet attained

a superior performance of 6.47% than the existing ResRandSVM classification model. In addition, the analysis utilizing TNR of the classification techniques is depicted in figure 10(b). The TSCO-L-LeNet recordedTNRof0.946, and the TNR obtained by existing leukemia classification techniques, like Enhanced incremental training is 0.817, Inception v3 XGBoost is 0.838, ResRandSVM is 0.885, and ECA-VGG16 is 0.904 for K-fold value 8. The evaluation proved that the TSCO-L-LeNet gained high performance of 4.46% than the ECA-VGG16 leukemia classification approach. Moreover, figure 10(c) displays the validation using accuracy of different classification models. Here, the TSCO-L-LeNet recorded accuracy for K-fold value 8 is 0.903. The prevailing leukemia classification approaches, such as Enhanced incremental training, Inception v3 XGBoost, ResRandSVM, and ECA-VGG16attained accuracy of 0.821, 0.845, 0.864, and 0.866. The validation results show that TSCO-L-LeNet measures increased performance of 9.08% as than traditional Enhanced incremental training model.

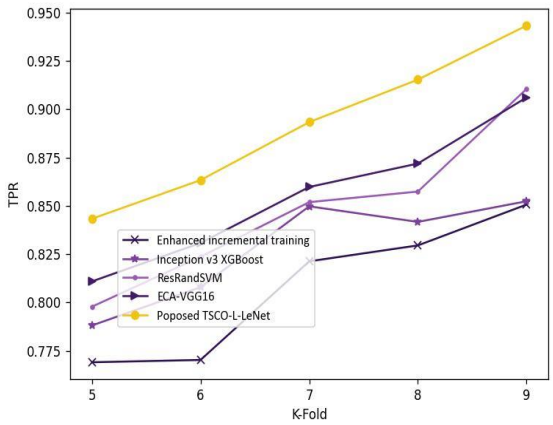

(a)

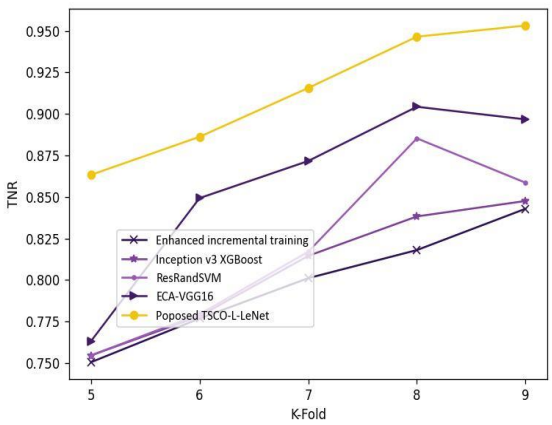

(b)

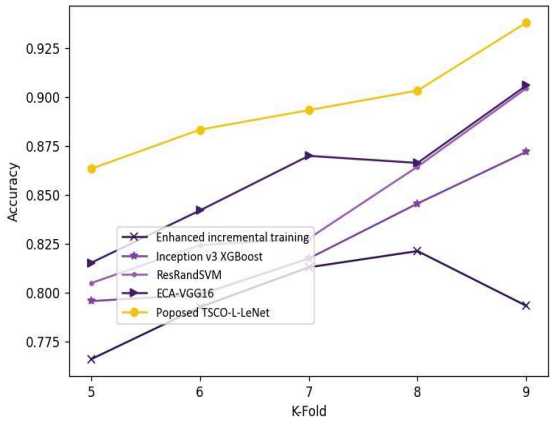

(c)

Figure 10. Comparative analysis of TSCO-L-LeNet utilizing K-fold ((a) TPR, (b) TNR, and (c) Accuracy

4.8. Comparative discussion

The results recorded during the investigation of superiority of TSCO-L-LeNet in leukemia classification are depicted in table 1. The superiority of TSCO-L-LeNet is identified by comparing the TSCO-L-LeNet with traditional classification models. The experimental results show that TSCO-L-LeNet attained best performance with maximum TPR, TNR, and accuracy of 92.22%, 91.47%, and 92.65% for 80% training data. Moreover, the existing classification models gained TPR of 83.43%, 83.61%, 84.94%, and 85.10% for Enhanced incremental training, Inception v3 XGBoost, ResRandSVM, and ECA-VGG16, which also recorded TNR of 83.43%, 83.61%, 84.94%, and 85.10%. In addition, the accuracy recorded by the existing classification models is 83.61%by Enhanced incremental training, 87.10%by Inception v3 XGBoost, 88.51% by ResRandSVM, and 88.73% by ECA-VGG16. In contrast, the L-LeNet models used for the classification of leukemia effectively utilized training parameters and increase the depth of learning to handle the long-term sequential data thus offering high performance during the classification task. Moreover, the classes that

negatively caused the network performance are accurately detected by employing incremental learning with L-LeNet model during classification.

Table 1. Comparative discussion

Variations	Parameters	Enhanced incremental training	Inception v3 XGBoost	ResRandSVM	ECA-VGG16	Proposed TSCO-L-LeNet
Training set (%)	**TPR (%)**	83.43	83.61	84.94	85.10	***92.22***
	TNR (%)	81.64	83.86	84.22	85.79	***91.47***
	Accuracy (%)	83.61	87.10	88.51	88.73	***92.65***
K-fold	**TPR (%)**	82.95	84.16	85.73	87.18	91.55
	TNR (%)	81.80	83.82	88.53	90.43	94.65
	Accuracy (%)	82.12	84.55	86.44	86.63	90.33

5. Conclusion

A hematologic form of cancer called leukemia occurs in the human body due to the increasing growth of abnormal WBC. It is essential to provide accurate treatment to patients with leukemia disease before causing severe impacts on one's life. This paper presents a novel optimization-based deep learning approach TSCO-L-LeNet for accurate classification of leukemia. The input blood smear images are pre-processed using an adaptive median filter and Scribble2label is utilized for the segmentation of pre-processed image. The segmented images are augmented and the different feature extractors are utilized for the extraction of relevant features from augmented image. The leukemia classification is performed finally using the L-LeNet model, here the optimal weights of L-LeNet are effectively fine-tuned by utilizing TSCO model. Later, incremental learning is performed on the leukemia classifier for incremental learning. Furthermore, the performance of TSCO-L-LeNet is validated with traditional leukemia classification approaches. The experimental result shows the TSCO-L-LeNet attained high performance with 92.22% of TPR, 91.47% of TNR, and 92.65% of accuracy. In future, the research will be further extended to analyze the classification performance of designed TSCO-L-LeNet using synthesized and large databases.

References

[1]Al-Qudah, R. and Suen, C.Y., “Improving blood cells classification in peripheral blood smears using enhanced incremental training”, Computers in Biology and Medicine, vol.131, pp.104265, 2021.

[2]Ramaneswaran, S., Srinivasan, K., Vincent, P.D.R. and Chang, C.Y., “Hybrid inception v3 XGBoost model for acute lymphoblastic leukemia classification”, Computational and Mathematical Methods in Medicine, pp.1-10, 2021.

[3] Sulaiman, A., Kaur, S., Gupta, S., Alshahrani, H., Reshan, M.S.A., Alyami, S. and Shaikh, A., “ResRandSVM: Hybrid Approach for Acute Lymphocytic Leukemia Classification in Blood Smear Images”, Diagnostics, vol.13, no.12, pp.2121, 2023.

[4]Zakir Ullah, M., Zheng, Y., Song, J., Aslam, S., Xu, C., Kiazolu, G.D. and Wang, L., “An attention-based convolutional neural network for acute lymphoblastic leukemia classification”, Applied Sciences, vol.11, no.22, pp.10662, 2021.

[5]Rodrigues, L.F., Backes, A.R., Travençolo, B.A.N. and de Oliveira, G.M.B., “Optimizing a deep residual neural network with genetic algorithm for acute lymphoblastic leukemia classification”, Journal of Digital Imaging, 35(3), pp.623-637.

[6] Saeed, U., Kumar, K., Khuhro, M.A., Laghari, A.A., Shaikh, A.A. and Rai, A., “DeepLeukNet-A CNN based microscopy adaptation model for acute lymphoblastic leukemia classification”, Multimedia Tools and Applications, pp.1-25, 2022.

[7]Baig, R., Rehman, A., Almuhaimeed, A., Alzahrani, A. and Rauf, H.T., “Detecting malignant leukemia cells using microscopic blood smear images: a deep learning approach”, Applied Sciences, vol.12, no.13, pp.6317, 2022.

[8]Das, P.K. and Meher, S., “An efficient deep convolutional neural network based detection and classification of acute lymphoblastic leukemia”, Expert Systems with Applications, vol.183, pp.115311, 2021.

[9]Jayasudha, S., “Comparision of preprocess techniques for brain image using machine learning”, Information Technology in Industry, vol.9, no.3, pp.653-656, 2021.

[10]Lee, H. and Jeong, W.K., “Scribble2label: Scribble-supervised cell segmentation via self-generating pseudo-labels with consistency”, In Proceedings of Medical Image Computing and Computer Assisted Intervention–MICCAI 2020: 23rd International Conference, Lima, Peru, October 4–8, 2020, Proceedings, Part I 23, Springer International Publishing, pp. 14-23, 2020.

[11]Zulpe, N. and Pawar, V., “GLCM textural features for brain tumor classification”, International Journal of Computer Science Issues (IJCSI), vol.9, no.3, pp.354, 2012.

[12]Guermoui, M. and Mekhalfi, M.L., “A Sparse Representation of Complete Local Binary Pattern Histogram for Human Face Recognition”, arXiv preprint arXiv:1605.09584, 2016.

[13]Bai, Y., Guo, L., Jin, L. and Huang, Q., “A novel feature extraction method using pyramid histogram of orientation gradients for smile recognition”, In Proceedings of 2009 16th IEEE International Conference on Image Processing (ICIP), IEEE, pp. 3305-3308, November 2009.

[14]Hung, T.Y. and Fan, K.C.,“Local vector pattern in high-order derivative space for face recognition”, In Proceedings of 2014 IEEE International Conference on Image Processing (ICIP), IEEE, pp. 239-243, October 2014.

[15]Xie, S., Shan, S., Chen, X. and Chen, J., “Fusing local patterns of gabor magnitude and phase for face recognition”, IEEE transactions on image processing, vol.19, no.5, pp.1349-1361, 2010.

[16]Wei, G., Li, G., Zhao, J. and He, A., “Development of a LeNet-5 gas identification CNN structure for electronic noses”, Sensors, vol.19, no.1, pp.217, 2019.

[17]Sagheer, A. and Kotb, M., “Time series forecasting of petroleum production using deep LSTM recurrent networks”, Neurocomputing, vol.323, pp.203-213, 2019.

[18]Layeb, A., “Tangent search algorithm for solving optimization problems”, Neural Computing and Applications, vol.34, no.11, pp.8853-8884, 2022.

[19]Seyyedabbasi, A. and Kiani, F., “Sand Cat swarm optimization: A nature-inspired algorithm to solve global optimization problems”, Engineering with Computers, pp.1-25, 2022.

[20] Blood Cells Cancer (ALL) dataset is taken from, “https://www.kaggle.com/datasets/mohammadamireshraghi/blood-cell-cancer-all-4class”accessed on October 2023.

[21] Khalifa, N.E., Loey, M. and Mirjalili, S., “A comprehensive survey of recent trends in deep learning for digital images augmentation”, Artificial Intelligence Review, pp.1-27, 2022.

[22] Ornek, A.H. and Ceylan, M., “Comparison of traditional transformations for data augmentation in deep learning of medical thermography”, In Proceedings of 2019 42nd International Conference on Telecommunications and Signal Processing (TSP), IEEE, pp. 191-194, 2019.

[23] Lessa, V. and Marengoni, M., “Applying artificial neural network for the classification of breast cancer using infrared thermographic images”, In Proceedings of Computer Vision and Graphics: International Conference, ICCVG 2016, Warsaw, Poland, September 19-21, 2016, Springer International Publishing, Proceedings 8, pp. 429-438, 2016.

[24] Su, R., Liu, T., Sun, C., Jin, Q., Jennane, R. and Wei, L., “Fusing convolutional neural network features with hand-crafted features for osteoporosis diagnoses”, Neurocomputing, vol.385, pp.300-309, 2020.

[25] Bhaladhare, P.R. and Jinwala, D.C., “A clustering approach for the-diversity model in privacy preserving data mining using fractional calculus-bacterial foraging optimization algorithm”, Advances in Computer Engineering, 2014.

[26] Mane, V.M. and Jadhav, D.V., “Holoentropy enabled-decision tree for automatic classification of diabetic retinopathy using retinal fundus images”, Biomedical Engineering/Biomedizinische Technik, vol.62, no.3, pp.321-332, 2017.